



Equivalence of cell survival data for radiation dose and thermal dose in ablative treatments: analysis applied to essential tremor thalamotomy by focused ultrasound and gamma knife

D. Schlesinger, M. Lee, G. ter Haar, B. Sela, M. Eames, J. Snell, N. Kassell, J. Sheehan, J. M. Larner & J. -F. Aubry

To cite this article: D. Schlesinger, M. Lee, G. ter Haar, B. Sela, M. Eames, J. Snell, N. Kassell, J. Sheehan, J. M. Larner & J. -F. Aubry (2017) Equivalence of cell survival data for radiation dose and thermal dose in ablative treatments: analysis applied to essential tremor thalamotomy by focused ultrasound and gamma knife, *International Journal of Hyperthermia*, 33:4, 401-410, DOI: [10.1080/02656736.2016.1278281](https://doi.org/10.1080/02656736.2016.1278281)

To link to this article: <https://doi.org/10.1080/02656736.2016.1278281>



Published online: 31 Jan 2017.



Submit your article to this journal [↗](#)



Article views: 1137



View related articles [↗](#)



View Crossmark data [↗](#)



Citing articles: 4 View citing articles [↗](#)

Equivalence of cell survival data for radiation dose and thermal dose in ablative treatments: analysis applied to essential tremor thalamotomy by focused ultrasound and gamma knife

D. Schlesinger^{a,c}, M. Lee^b, G. ter Haar^d, B. Sela^b, M. Eames^b, J. Snell^{b,c}, N. Kassell^{b,c}, J. Sheehan^{a,c}, J. M. Larner^a and J. -F. Aubry^{a,e}

^aDepartment of Radiation Oncology, University of Virginia, Charlottesville, VA, USA; ^bFocused Ultrasound Foundation, Charlottesville, VA, USA; ^cDepartment of Neurosurgery, University of Virginia, Charlottesville, VA, USA; ^dDivision of Radiotherapy and Imaging, The Institute of Cancer Research:Royal Marsden Hospital, London, UK; ^eESPCI Paris, PSL Research University, CNRS, INSERM, Institut Langevin, Paris, France

ABSTRACT

Thermal dose and absorbed radiation dose have historically been difficult to compare because different biological mechanisms are at work. Thermal dose denatures proteins and the radiation dose causes DNA damage in order to achieve ablation. The purpose of this paper is to use the proportion of cell survival as a potential common unit by which to measure the biological effect of each procedure. Survival curves for both thermal and radiation doses have been extracted from previously published data for three different cell types. Fits of these curves were used to convert both thermal and radiation dose into the same quantified biological effect: fraction of surviving cells. They have also been used to generate and compare survival profiles from the only indication for which clinical data are available for both focused ultrasound (FUS) thermal ablation and radiation ablation: essential tremor thalamotomy. All cell types could be fitted with coefficients of determination greater than 0.992. As an illustration, survival profiles of clinical thalamotomies performed by radiosurgery and FUS are plotted on a same graph for the same metric: fraction of surviving cells. FUS and Gamma Knife have the potential to be used in combination to deliver a more effective treatment (for example, FUS may be used to debulk the main tumour mass, and radiation to treat the surrounding tumour bed). In this case, a model which compares thermal and radiation treatments is valuable in order to adjust the dose between the two.

ARTICLE HISTORY

Received 25 April 2016
Revised 28 December 2016
Accepted 28 December 2016
Published online 23 January 2017

KEYWORDS

Ultrasound; thermal dose; radiation dose; damage index; high intensity focused ultrasound

Introduction

Therapies involving the use of ionising radiation and/or thermal energy have a long history in the treatment of disease, including cancer. Evidence from an Egyptian papyrus suggests that as early as 3500 years ago heat was applied in an attempt to treat breast cancer [1,2]. Therapy involving radiation had to wait until the discovery of X-rays in 1895, however within several years of this discovery, radiation therapy based on radionuclides and low-energy X-ray generating equipment was used for the treatment of cancer [3]. More recently, there have been parallel developments in the use of heat and ionising radiation for both diffuse and focal disease, as well as attempts to combine the benefit of the two modalities. A number of techniques have been developed to allow the focal destruction of malignant tissue in humans, including ablation by radiofrequency [4], microwaves [5–12], lasers [13], magnetic nanoparticles [14,15] and high-intensity focused ultrasound [16–18]. Recent advancements in the focal treatment of cancer using ionising radiation include the development of stereotactic radiosurgery (SRS) [19],

stereotactic body radiotherapy (SBRT) [20–22] and intraoperative radiotherapy (IORT) [23,24].

From an early date and continuing to the present, investigation of the synergies between heat and ionising radiation has been a natural avenue for research including the basic biology of hyperthermia [25], the most effective sequencing of heating and radiation [26,27], biological interactions between heat and radiation [28] and determination of thermal enhancement ratios and predictors of response [28–30]. Significant evidence in the form of several randomised control trials exists to demonstrate that hyperthermia followed by radiation can significantly improve outcomes in head and neck cancer [31,32], malignant melanoma [33], breast cancer [34], glioblastoma multiforme [35], pelvic tumours [36], cervical carcinoma [37], superficial tumours [38], cervical cancer [39], non-small-cell lung cancer [40], rectal cancer [41] among others [2,42]. The recent progress in focal ablative therapies such as HIFU and SRS/SBRT may also benefit from combined approaches. However, direct comparison of absorbed dose in ionising radiation and thermal dose for heating have

historically been difficult because of the widely different physical and biological mechanisms in play [1].

In this work, we compare thermal and ionising radiation modalities in terms of biological damage to tissue by using equivalent historical *in vitro* cell survival data. By doing so, we aim to create a method for translation between measures of thermal and radiation dose. Essential tremor thalamotomy is currently the only indication for which quantitative clinical data are available for both radiation and FUS treatments. In order to illustrate this approach, we thus took into account the beam-shaping capabilities of the stereotactic radiosurgery (SRS) and FUS devices available for treatment of essential tremor, in order to allow more direct comparison between FUS and SRS treatments. Our approach could facilitate dosimetry planning in the setting of combined radiosurgery and FUS.

Biological effect of ionising radiation and definition of radiation dose

Photon-based ionising radiation (X-rays and γ -rays) are indirectly ionising; they deposit energy in tissue in a two-step process. In the first step, photoelectric and Compton interactions between photons and atoms in tissue result in the transfer of energy to fast electrons ejected from the target atoms. In a second step, atoms in the targeted tissue are ionised as these fast electrons undergo Coulomb interactions with other atoms in the targeted tissue, transferring a fraction of their energy during each interaction [43]. In traditional radiobiology theory, the biological target of ionising radiation is damage to DNA. In a minority of cases (~33%), DNA is directly ionised, leading to strand breaks. In the majority of cases (~66%), the ions created in irradiated tissue result in the creation of free radicals (most significantly hydroxyl radicals) which subsequently react with and create strand breaks in DNA. The ultimate biological effect of the DNA damage is mitotic death of the cells in the irradiated tissue [1]. At higher, ablative doses there may additional biological mechanisms at play as well, including microvascular damage [44].

Radiation dose is described in physical terms: the amount of energy absorbed per mass of tissue. This is the definition of “absorbed dose”, and is most commonly assigned units of Gray (Gy), where 1 Gy = 1 J/kg of energy absorbed in tissue [43]. The amount of biological damage caused can be related directly to the physical quantity of absorbed dose, and this has become the standard method of prescribing the appropriate amount of radiation to be delivered in any given therapeutic setting.

Biological effect of thermal energy and definition of thermal dose

The response of cells to thermal insult at sub-ablative temperatures (such as temperatures employed in traditional hyperthermia) can be quite complex, involving the development of a combination of thermotolerance, cytotoxicity and radiosensitisation most likely mediated by protein

denaturation within cells which increases proportionately to the thermal damage. Lower level of protein denaturation can trigger protective mechanisms such as increased expression of heat shock proteins which help to stabilise the cell against further thermal damage. Higher levels of protein denaturation can cause the inactivation of protein synthesis and DNA repair mechanisms resulting in cytotoxicity and increased sensitivity to ionising radiation [45]. When delivered at sufficient power to result in ablation, thermal energy ultimately results in coagulative necrosis [46]. As with ionising radiation, the extent of biological changes in tissue resulting from thermal exposure is correlated with the amount of energy absorbed in tissue. However, for thermal energy, it is the temperature to which the tissue is raised, and the duration of the heating that seem to play the predominant biological role. Sapareto and Dewey have defined a “thermal isoeffective dose” [47]. This has units of cumulative equivalent minutes at 43°C (CEM 43°C), and allows conversion of any temperature/time (T/t) combination to the equivalent time for which the reference temperature of 43°C must be applied to obtain the same level of thermal damage:

$$\text{CEM}_{43} = \int_0^t R^{43-T(t)} dt$$

$$R = \begin{cases} 0.25 & \text{if } T < 43^\circ\text{C} \\ 0.5 & \text{if } T > 43^\circ\text{C} \end{cases}$$

The definition of the thermal isoeffective dose formalises the idea that two different temperatures applied over different time intervals can have the same biological effect in a given tissue.

Cell survival curves

Traditionally, the most common method for assessing cell survival in thermo- and radiobiology uses survival curves. The principle of survival curve analysis is the same, irrespective of the source of cell damage. The curve depicts the relationship between the damage to which a cell has been subjected and the cell's subsequent ability to divide to form a colony. For the studies considered here, *in vitro* assays have been used as the source data. The development of survival curves involve plating a known number of cells (determined using a standard counting method) out into tissue culture dishes following exposure to heat or ionising radiation, and analysing their response at a later time point. The surviving fraction is calculated by normalising the number of cells or colonies seen in treated samples to that seen in controls. This is then plotted on a logarithmic scale against the thermal or radiation dose delivered [1]. A minimum colony size (usually 50 cells) is used as a cut-off for minimal critical mass of cells to survive as a colony. It should be noted, that while this type of assay is frequently assumed to measure individual cell survival directly, the reduction in number after treatment may also be due in part to cells going into a “dormant” state, and not dividing [1]. Typical survival curves are shown in Figure 1 for radiotherapy and thermal doses. For thermal treatments, the cells

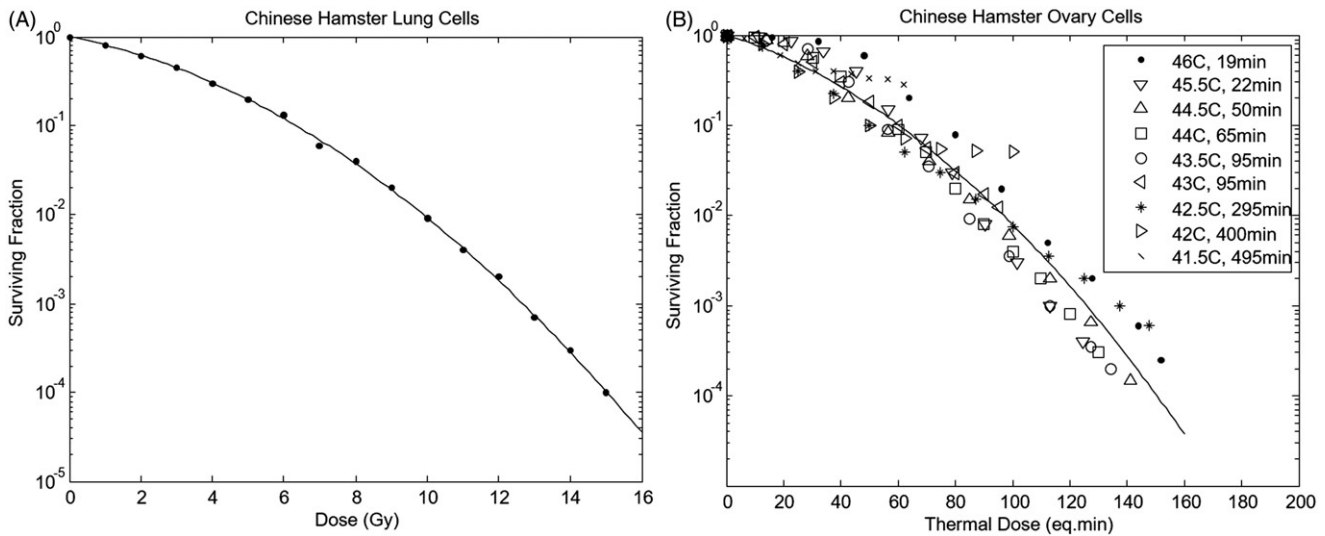


Figure 1. An example of a survival curve for radiotherapy exposure (A), extracted from [97], and for heated cells (B), extracted from previously published results [98], with thermal isoeffective dose calculated from the combination of heating duration and temperature.

were subjected to a variety of temperatures as shown in the figure legend. However, when both temperature and time are taken into account by calculating thermal dose in CEM, the data fall along a common curve.

Materials and methods

Literature review

An extensive review of the literature was conducted to identify studies reporting cell survival for thermal exposure, with the goal of identifying cell subtypes for which there were matching published reports on cell survival for ionising radiation. Basically a literature review for both thermal and radiation cell survival was performed and then data were cross referenced. The literature review was conducted using Cornell University's online library during June and July of 2013. Keywords used in this literature review included: cell survival, radiation treatment, thermal treatment, thermal dose, radiation dose, tissue damage and hyperthermia. Some exclusion criteria included: articles not written in English, studies that only used thermal and radiation treatment in combination and studies that did not measure cell survival. Table 1 lists the publications selected for thermal and ionising radiation modalities. The list is not exhaustive and the literature search was stopped when three different cell-types were found for which survival data were available: Chinese hamster ovary cells (CHO), Chinese hamster lung cells (CHL) and human glioblastoma tumour cells will thus be used in the rest of the article to illustrate our approach.

Data extraction and cell survival modelling

Each point of the survival data, as displayed in the reports selected for thermal and ionising radiation experiments, was manually transferred into Matlab version R2013a (Mathworks, Inc., Natick, MA) for each cell type: CHO, CHL and human glioblastoma astrocytoma (GBA). The radiation dose survival profiles for each of the three cell types were modelled using

the Universal Survival Curve (USC) developed by Park et al. [48]. The USC is one of several derivatives of the linear quadratic model that attempt to take into account low and high doses survival regimes [44,49–53]:

$$\ln S = \begin{cases} -n(\alpha * D_r + \beta * D_r^2) & \text{for } D_r \leq D_T \\ -n \left(\frac{1}{D_o} D_r - \frac{D_q}{D_o} \right) & \text{for } D_r \geq D_T \end{cases}$$

where, S is the cell survival, defined as the ratio between the remaining number of undamaged cells at time t indicated by $N(t)$ to the number of undamaged cells $N(0)$ present prior to the start of the treatment, D_r is the radiation dose in Gray, n is the number of fractionations and α (units of \log_e of cells killed per Gy) and β (units \log_e of cells killed per Gy^2) are constants that describe the linear and quadratic portions of the curve, respectively. D_T is the transition dose, where the curve changes from using the low-dose model to the high dose. D_o is a measure of the slope of the linear portion of the curve at high doses and D_q is the x-intercept of the survival line valid for $D_r \leq D_T$. β and D_T are calculated from the parameters α , D_o , and D_q to ensure continuity and differentiability at D_T [48]:

$$\beta = \frac{(1 - \alpha * D_o)^2}{4D_o * D_q}$$

$$D_T = \frac{2 * D_q}{1 - \alpha * D_o}$$

In traditional radiobiology, the α and β terms above are also often represented in ratio form (the α/β ratio, units of Gy), which is the dose at which the linear and quadratic components are equal. Tumours and tissue which show an early response to radiation damage tend to have a large α/β ratio, while tissue which shows a late response to radiation damage have a small α/β ratio [1,53,54]. Thermal dose survival data were fitted with a linear-quadratic equation for all three cell types [55,56]:

$$S = e^{-(aD_t + bD_t^2)}$$

Table 1. Review of papers reporting survival of cells exposed to thermal rise or ionising radiations, matched for cell subtype and dose range.

Reference article	Type of tissue investigated		Treatment modality	Dose range
Sensitivity of Human Cells to Mild Hyperthermia [43]	Human Glioblastoma Tumour Cells	U87MG	Heat	0–240 CEM
Thermal Dose Determination in Cancer Therapy [42]	Chinese Hamster Ovary		Heat	0–150 CEM
Cellular Effects of Hyperthermia: Relevance to the minimum dose for thermal damage [44]	Chinese Hamster Lung	V79	Heat	0–150 CEM
Arrhenius Relationships from the Molecule and Cell to the Clinic [45]	Chinese Hamster Ovary		Heat	0–150 CEM
Basic Principles of thermal dosimetry and thermal threshold for tissue damage from hyperthermia [46]	Chinese Hamster Ovary		Heat	0–180 CEM
A Transient Thermotolerant Survival Response Produced by Single Thermal Doses in HeLa Cells [47]	HeLa		Heat	0–480 CEM
Differential Effect of Hyperthermia on Murine Bone Marrow Normal Colony-forming Units and AKR and L1210 Leukemia Stem Cells [48]	Leukaemia Cells	L1210, AKR	Heat	0–60 CEM
A Comparison of Cell Killing by Heat and/or X Rays in Chinese Hamster V79 Cells, Friend Erythroleukemia Mouse Cells, and Human Thymocyte MOLT-4 [49]	Chinese Hamster Lung	V79	Radiation	0–16 Gy
Cellular Responses to Combinations of Hyperthermia and Radiation [50]	Chinese Hamster Ovary		Radiation	0–11 Gy
Cross-Resistance to Ionizing Radiation in a Murine Leukemic Cell Line Resistant to cis-Dichlorodiammineplatinum(II): Role of Ku Autoantigen [51]	Leukaemia Cells	L1210	Radiation	0–10 Gy
Effect of Hyperthermia on the Radiation Response of two Mammalian Cell Lines [52]	Chinese Hamster Ovary, mouse mammary sarcoma	HA-1, EMT-6	Radiation	0–12 Gy
Effects of propranolol in combination with radiation on apoptosis and survival of gastric cancer cells in vitro [53]	Human gastric adenocarcinoma cells	BGC-823, SGC-7901	Radiation	0–10 Gy
Enhancement of Radiation Damage in Cellular DNA Following Unifilar Substitution with Iododeoxyuridine [54]	Chinese Hamster Lung	V79	Radiation	0–16 Gy
Hyperthermia Radiosensitization in Human Glioma Cells Comparison of Recovery of Polymerase Activity, Survival, and Potentially Lethal Damage Repair [55]	Human Glioblastoma Tumour Cells	U87MG	Radiation	0–12 Gy
Influence of Hyperthermia on Gamma-Ray-Induced Mutation in V79 Cells [56]	Chinese Hamster Lung	V79	Radiation	0–12 Gy
Interaction of Hyperthermia and Radiation in CHO Cells: Recovery Kinetics [57]	Chinese Hamster Ovary		Radiation	0–12 Gy
Long duration mild temperature hyperthermia and brachytherapy [58]	Human Normal fibroblasts, Human radiation resistant melanoma cells, Human Ovarian Carcinoma cells	AG1522, SkMe13, A2780	Radiation	0–10 Gy
Moderate Hyperthermia and Low Dose Irradiation [59]	Chinese Hamster Lung	V79	Radiation	0–14 Gy
Radiosensitivity and Capacity to Recover from Radiation Induced Damage in Pimonisazol-Unlabeled Intratumor Quiescent Cells Depend on p53 Status [60]	Human head and neck squamous carcinoma cells	SAS	Radiation	0–14 Gy
Recovery of Sublethal Radiation Damage and its inhibition by Hyperthermia in normal and transformed mouse cells [61]	Chinese Hamster Lung	V79	Radiation	0–14 Gy
The p65 subunit of nuclear factor- κ B is a molecular target for radiation sensitization of human squamous carcinoma cells [62]	Human head and neck squamous carcinoma cells	SCC-35, d6, d12	Radiation	0–11 Gy
Thermal radiosensitization in Chinese hamster and mouse C3H 10T 1/2 cells. The thermotolerance effect [60]	Chinese Hamster Lung, mouse embryo	V79, C3H	Radiation	0–14 Gy
Thermal Sensitivity and Radiosensitization in V79 Cells after BrdUrd or IdUrd Incorporation [63]	Chinese Hamster Lung	V79	Radiation	0–16 Gy
Thermally Enhanced Radioresponse of Cultured Chinese Hamster Cells: Inhibition of Repair of Sublethal Damage and Enhancement of Lethal Damage [64]	Chinese hamster fibroblasts	V79	Radiation	0–11 Gy
Dose rate: Its effect on the survival of HeLa cells irradiated with gamma rays [65]	HeLa	S3	Radiation	0–10 Gy
Variations in several responses of HeLa cells to X-irradiation during the division cycle [66]	HeLa	S3	Radiation	0–10 Gy
Action of radiation on mammalian cells, IV. Reversible mitotic lag in the S3 HeLa cell produced by low doses of X-rays [67]	HeLa	S3	Radiation	0–10 Gy
Thermal sensitivity and radiosensitization in Chinese hamster V79 cells exposed to 2-aminopurine or 6-thioguanine [68]	Chinese Hamster Lung	V79	Radiation	0–14 Gy

where, S is the cell survival, D_t is the thermal dose in equivalent minutes and a and b are constants.

Damage index Ω is widely used for RF and laser ablation. It is the logarithm of the ratio between the number of undamaged cells $N(0)$ present prior to the start of the treatment to the remaining number of undamaged cells at time t indicated by $N(t)$ [57]:

$$\Omega = \ln \frac{N(0)}{N(t)} = \ln \frac{1}{S}$$

Ω can thus be expressed as a function of the thermal dose with the same fit coefficients a and b calculated above:

$$\Omega = aD_t + bD_t^2$$

Evaluation of clinical treatment spot sizes

For sake of illustration, clinical data from both radiation surgery and thermal ablation have been processed. The only indication which the authors could get access to data sets for both is essential tremor. Thalamotomy data for both FUS and SRS were thus analysed for predicted cell survival. The clinical data used for analysis are anonymised data from a pilot study for essential tremor patients conducted at the University of Virginia [58] under oversight and approval of the university's Institutional Review Board (IRB). The anonymised Gamma Knife SRS dose distributions for the three cases used in the analysis have been determined by the IRB to be not subject to IRB review.

Focused ultrasound

The clinical FUS study consisted of 15 patients with essential tremor whose condition did not improve with medication. The patients were treated with MR-guided FUS, targeting the ventral intermediate (VIM) nucleus of the thalamus. A series of low-power sonications were delivered to the intended target to validate the geometric accuracy of the set-up.

Temperature maps were recorded during treatment using MR thermometry [59]. In this study, the temperature for each

voxel was read from the raw data files for each timepoint of the sonication and used to calculate the thermal dose. The thermal dose profile was determined by normalising the data to the maximum thermal dose in the volume of interest.

Using the calculated thermal profiles and the cell survival-thermal dose relationship for all cell lines (CHO, CHL and GBA), cell survival was calculated for each voxel in the region of interest.

Gamma knife radiosurgery

The clinical radiosurgery data are derived from treatment plans for three radiosurgical thalamotomies performed on the Gamma Knife at University of Virginia for individuals with essential tremor that have failed to improve with other treatments and are unwilling, or unable, to undergo an invasive procedure. Radiosurgical thalamotomy was achieved using the Leksell Gamma Knife to deliver a maximum dose of 130–140 Gy with a 4 mm isocenter to the VIM nucleus on the opposite side of the brain from the more severe tremor. The technique employed at the University of Virginia is similar to techniques published in the literature [60].

SRS dose distributions were created using the Gamma Knife treatment planning software (Leksell GammaPlan versions 8.0–10.1, Elekta AB, Stockholm). The resulting dose distributions were exported in anonymised DICOM-RT format. The radiotherapy dose profiles in x and y directions were averaged and then normalised to the maximum administered dose and converted to a percentage. Using the cell survival-radiotherapy dose relationship for CHO, CHL and GBA, the fraction of cells surviving was determined as a function of distance.

Results

Cell survival fitting

The resulting cell survival curves, extracted from previous studies, [61–66] are shown in Figure 2 for radiotherapy and thermal dose.

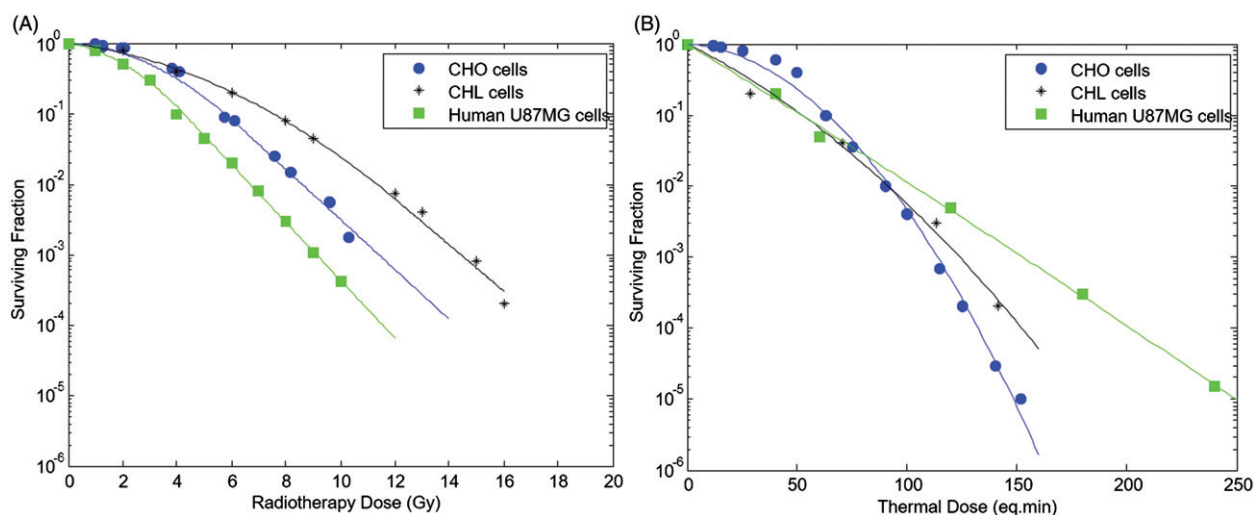


Figure 2. Fraction of cells surviving as a function of the radiation (A) or thermal (B) dose for (●) CHO, (◆) CHL and (■) GBA. Data have been extracted from previously published results: (CHO), [61] (CHL), [62] (GBA) [65] (A) and (CHO), [63] (CHL), [66] (GBA) [64] (B).

Table 2. Parameters for the Universal Survival Curve (USC) for radiation therapy doses and linear quadratic exponential fit for thermal doses.

USC fit (radiation dose)	α (1/Gy)	β (1/Gy ²)	α/β (Gy)	D_q (Gy)	D_o (Gy)	D_T (Gy)	R^2
CHO	0.043	0.062	0.69	2.93	1.23	6.19	0.993
CHL	0.11	0.026	4.12	5.23	1.33	12.22	0.995
GBA	0.14	0.094	1.53	1.81	1.06	4.28	0.996
Exponential fit (thermal dose)	a (1/CEM)		b (1/CEM ²)		a/b (CEM)		R^2
CHO	0.0047		0.00049		9.6		0.994
CHL	0.035		0.00017		210		0.992
GBA	0.044		9.1e-6		4800		0.998

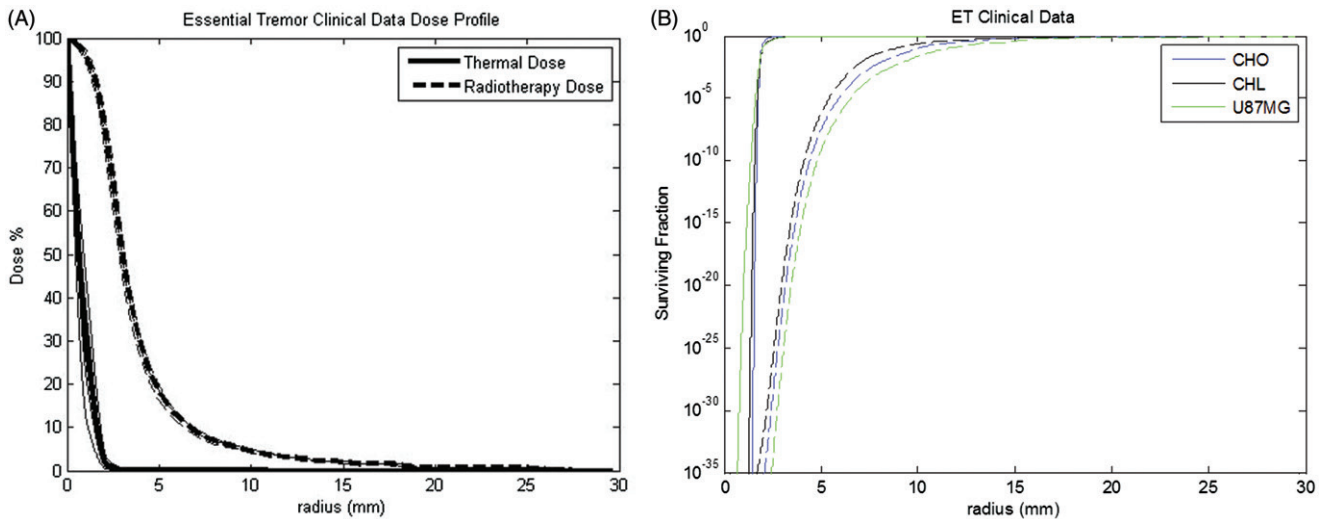


Figure 3. Average dose profiles (A) and corresponding survival curves (B) for essential tremor clinical data. The average profiles amongst patients are shown in four directions from the centre and the average is highlighted in bold (A). Survival curves for essential tremor clinical data for FUS (solid) and SRS (dashed) are plotted for each cell type available.

Results are summarised in Table 2. The α/β values for the radiation treatment on the 3 types of cells are close to previously published values [54,67,68]. The linear quadratic fit of the curves resulted in an average coefficient of determination of $R^2=0.995$, a maximum of 0.998, and a minimum of 0.992. All R^2 values are displayed in Table 2. In order to achieve a cell survival fraction of 10^{-5} (i.e. a survival of 0.001%), a radiotherapy dose of 17 Gy must be applied to CHO cells, 20.5 Gy to CHL cells, and 14 Gy to GBA cells. To achieve the same percentage of surviving cells a thermal dose of 148.5CEM must be administered to the targeted CHO cells, 178CEM to CHL cells, and 249.5CEM to GBA cells.

Estimated cell survival from clinical MRgFUS and Gamma Knife essential tremor treatments

The dose profiles from the clinical essential tremor data for FUS and SRS are shown in Figure 3(A), normalised to the point of maximum delivered dose (3160 CEM for thermal and 130 Gy for SRS). About 10% of the maximum dose is delivered to cells at 1.6 mm for thermal dose and at 6.9 mm for radiotherapy exposures. As seen in the simulated profiles, the thermal dose profile drop off is sharp and by 3 mm the dose is at zero. For the radiotherapy dose, the drop off is much more gradual and reaches an average of 4% of the maximum dose at 11 mm.

The corresponding simulated cell survival curves for the essential tremor clinical data are displayed in Figure 3(B). As an example, for GBA cells, the survival curve for the radiotherapy dose clinical data reaches a level of 90% at 28.9 mm and 99.5% at 27.78 mm. For the thermal dose, 90% survival occurs at a distance of 3.71 mm and reaches 99.5% survival at a distance of 6.5 mm. The survival curve for radiotherapy dose drops off more gradually than the thermal dose survival curve (Figure 3A).

Discussion

Potential clinical applications of FUS overlap significantly with SRS. FUS is being considered as a substitute modality for radiotherapy for indications such as essential tremor, neuropathic pain and others. However, the techniques do not need to compete. A more common scenario may be to use FUS in combination with radiotherapy, especially in the treatment of malignant disease. In this setting, FUS may be used to debulk the main tumour mass, allowing for significant and immediate symptomatic relief. This may be followed by radiation to the surrounding tumour bed with the goal of reducing local failure and regional recurrences. Investigators are also looking at the reverse approach, where the tumour and the surrounding tumour bed are first irradiated to damage the ability of the cells to reproduce. This is then followed by FUS to debulk the main tumour.

In either situation, a method of quantifying the biological damage inflicted on both normal and diseased tissue from both modalities, like the one introduced in this paper, would be valuable, and in particular for areas of tissue receiving sub-lethal doses from either modality on its own.

Historically, creating a direct comparison between thermal dose and radiation dose has been considered impractical [1]. This is in part because the concept of absorbed dose for ionising radiation describes the physics of the situation; i.e. the energy absorbed by a mass of tissue from exposure to ionising radiation [43]. Conversely, the formulation of the thermal iso-effective dose is based on empirically observed effects in heated cells.

However, SRS [19] and FUS surgery [16,69] attempt to achieve a similar biological effect: the ablation of a volume of tissue. SRS, especially when delivered in a single fraction, delivers a dose to tissue that can be considered “ablative” in the sense that the expected surviving fraction of cells is low [70]. Likewise, FUS achieves ablation of a desired region of tissue by heating to a thermal isoeffect dose known to cause coagulative necrosis with a similarly negligible surviving cell fraction [71,72]. A threshold for damage of 240CEM was determined *in vivo* in dog prostate [73] and in muscle [74] and corresponds to the threshold used in most clinical systems [75]. Normalisation to a similar biological endpoint makes feasible a direct comparison of radiation dose and thermal isoeffect. The threshold thermal or radiation dose required to “just” achieve ablation gives us a sort of “calibration” point in the spectrum of biological damage at which to equate the two dose formulations.

Equating the dose formulations might benefit the planning of combination therapies which take advantage of the synergistic effect of radiotherapy and thermal ablation. Compared to RF ablation alone, RF ablation combined with radiation therapy has been shown to increase the ablation volume in rat tumours [76] and improve survival [77], has shown a low rate of complications in patients with unresectable lung cancer [78–80] and has increased the relapse-free survival rate in prostate adenocarcinoma [81]. This pioneering work could be revisited in an optimal way by taking advantage of the non-invasive and conformal treatment capabilities of focused ultrasound and external beam therapy for inducing thermal and radiation effects with 3D planning based on the cell survival formulation proposed here.

The thermal energy resulting in cytotoxicity drops off faster than for radiation therapy (Figure 3). In part, this is related to the physics and technical details of the devices. Gamma Knife, used as a platform for the radiosurgery dose distributions in our study, achieves a steep dose profile through the application of a large number (192 in the Perfexion model Gamma Knife used in this study) cross-firing beams that are collimated so they intersect with high precision at a focal point. A single irradiation location or “isocenter” creates an approximately spherical dose distribution. Irradiation of irregularly shaped targets is achieved by using multiple isocenters and collimator settings at different positions. The dose falloff on a Gamma Knife is fundamentally dependent on the attenuation of each beam (which is at 60Co energy), the penumbra of each beam and the total

number of beams, and the isodose level in the distribution placed at the treatment margin of the target [82]. The sharper spatial distribution falloff of the thermal dose is linked to the size of each individual heated region (focal spot) and thus to the ultrasonic transducer geometry, and the frequency used. This is not unexpected as thermal conduction is a very inefficient method of heating tissue [83]: thermal conduction is an inherent limitation for large treatment volumes with focused ultrasound as the focal spot is small. The whole volume needs to be treated spot by spot. Nevertheless, limited diffusion can also be seen as an advantage as it contributes to a sharper boundary and a better control of energy deposition.

Limitations of this study

The intent of this paper was to explore the potential utility of equating thermal dose and radiation dose effects using cell survival as a common unit of measurement. As there is limited data collected with the intent of making such a direct comparison, there are assumptions that impact the uncertainties in the analysis including the *in vitro* cell survival data used in the study, the accuracy of survival models at ablative doses and simplification of the possible complexities of the joint biological effects of thermal energy and ionising radiation.

Limitations of *in vitro* cell survival data in this study

Perhaps the most significant limitation of our experiment is that *in vitro* studies do not represent clinical reality. By design, *in vitro* experiments use cells grown under carefully controlled conditions. The *in vivo* situation is obviously much more complex; for example, our models do not take into account the heat sink effect of the surrounding tissue vasculature [84], cell-cycle differences [85] or tissue inhomogeneities which can distort thermal and radiation dose [86–88]. Stochastic models have shown that time-temperature history, tumour geometry, tumour perfusion and uniformity of heating are all likely to affect cell survival rates [89]. Nor do *in vitro* models account for immunological effects, inflammatory effects, chemokines or cytokines that are present *in vivo* [90,91]. In addition, the cell lines used to create the thermal dose and radiation dose survival curves in this paper do not correspond with the cell types (i.e. normal brain tissue) irradiated during a FUS thalamotomy or radiosurgery thalamotomy. This was because of the non-existence of published data for our chosen clinical example. The mismatch between *in vitro* cell lines and the cells found in human brain tissue creates uncertainties on the specific parameters determined for our model fit. As *in vitro* and *in vivo* cell survival data are accrued for thermal and radiation doses over a larger range of cell-types, the method presented in this paper can be refined to include better parameter estimates.

Limitations of survival models at ablative doses

Another limitation to our approach is that the mathematical models used for thermal and radiation dose derive from

in vitro cell survival data acquired at sub-ablative doses. Both the thermal dose and ionising radiation cell survival models have been shown to have weaknesses at high, single-fraction doses. Ideally, experiments should be conducted on the same types of cells, with the same cell survival assay and for SRS-like doses. Multiple models for thermal damage and radiation damage could also be employed to better represent the likely uncertainty in the calculations [92]. This is beyond the scope of the present paper.

Simplifying assumptions regarding the joint biological effects of thermal energy and ionising radiation

A simplifying assumption of the study is that thermal dose and radiation dose may be treated independently. In practice, there is likely some degree of interaction between the two. For instance, hyperthermia studies have demonstrated *in vitro* that the achievable radiosensitisation caused by heating is dependent on the sequence and time interval between heating and irradiation. While data remain inconclusive, there is a consensus that simultaneous heating and irradiation would maximise the dose enhancement effect due to heat, and as the interval between heat and radiation increases (regardless of sequence) the degree of enhancement decreases [26]. Radiosensitisation may also be enhanced through heating by preferentially killing chronically hypoxic tissue as is often found in the centre of malignant tumours as they grow. These hypoxic regions tend to be radioresistant, and it is unclear how using heat to destroy these regions would effect the overall sensitivity profile to a joint treatment. A related effect is that heating can cause increased perfusion to targeted tissue, helping to reoxygenate (and thus radiosensitise) hypoxic areas of tissue [93,94].

This study attempts to relate thermal dose and radiation dose at a very low “ablative” level of cell kill, perhaps avoiding some of the complexities of the interactions between the biology of thermal and radiation insults. The thermal dose profiles presented in the results include a thin region of sub-lethally heated tissue. This tissue likely benefits from some of the radiosensitisation that has been demonstrated from these earlier hyperthermia results, and this is not accounted for in our model. However further investigation will be required to understand what, if any, clinical significance these sub-lethally heated regions would have on the ultimate outcome of a joint thermal/radiation treatment and how it might affect thermal or radiation dose prescriptions.

Other limitations of the work

Finally, different tissue and organ types have differential sensitivity to both ionising and thermal dose. This is also not modelled in the current approach, however it is inherent in the *in vitro* cell data used in the study. Differential response to ionising radiation is partly related to the length of the cell-cycle of a given cell type, as lethal DNA damage is manifested during mitosis. Cells with short lifespans tend to show early reaction to radiation insult. Slower-dividing cells tend to show later reactions [1]. The primary mechanism of thermal cell death is a combination of protein denaturation and

coagulative necrosis. This could reasonably be assumed to be similar across all cell lines. The differences then may be due to alternative mechanism of cell death such as disruption of intracellular signal transduction and cell motility [42,95,96].

Conclusions

Radiation- and thermal-based treatments are difficult to compare because of the differences in the physics of the energy deposition and the resulting biological effects. The work presented in this paper is a first attempt at creating a method of equating thermal and radiation doses for ablative treatments by considering “ablation” as a common biological endpoint. It was shown how radiation dose and thermal dose could both be expressed in terms of percentage of surviving cells, and thus be compared with the same quantitative effect on tissues. Much work remains to be done in order to validate the regression equations and dose models against both *in vitro* and *in vivo* targets of different heterogeneous tissues.

Disclosure statement

Neal Kassell is an InSightec shareholder. The authors alone are responsible for the content and writing of the article.

References

- [1] Hall EJ, Giaccia AJ. (2006). Radiobiology for the radiologist Philadelphia (PA): Lippincott Williams&Wilki.
- [2] Horsman MR, Overgaard J. (2007). Hyperthermia: a potent enhancer of radiotherapy. Clin Oncol (R Coll Radiol) 19:418–26.
- [3] Lederman M. (1981). The early history of radiotherapy: 1895-1939. Int J Radiat Oncol Biol Phys 7:639–48.
- [4] Haemmerich D. (2010). Biophysics of radiofrequency ablation. Crit Rev Biomed Eng 38:53.
- [5] Carrafiello G, Ierardi AM, Fontana F, et al. (2013). Microwave ablation of pancreatic head cancer: safety and efficacy. J Vasc Interv Radiol 24:1513–20.
- [6] Chen JC, Moriarty JA, Derbyshire JA, et al. (2000). Prostate cancer: MR imaging and thermometry during microwave thermal ablation-initial experience. Radiology 214:290–7.
- [7] Healey TT, Dupuy DE. (2012). Microwave ablation for lung cancer. Med Health R 95:52–3.
- [8] Kuang M, Lu MD, Xie XY, et al. (2007). Liver cancer: increased microwave delivery to ablation zone with cooled-shaft antenna—experimental and clinical studies. Radiology 242:914–24.
- [9] Skinner MG, Iizuka MN, Kolios MC, et al. (1998). A theoretical comparison of energy sources - microwave, ultrasound and laser - for interstitial thermal therapy. Phys Med Biol 43:3535.
- [10] Vargas HI, Dooley WC, Gardner RA, et al. (2004). Focused microwave phased array thermotherapy for ablation of early-stage breast cancer: results of thermal dose escalation. Ann Surg Oncol 11:139–46.
- [11] Yoshitani S, Hayashi K, Kuroda M, et al. (2005). [Results of local ablation therapy for liver metastases from colorectal cancer using radiofrequency ablation and microwave coagulation therapy (RFA/MCT)]. Gan to Kagaku Ryoho 32:1666–9.
- [12] Zhang X, Chen B, Hu S, et al. (2008). Microwave ablation with cooled-tip electrode for liver cancer: an analysis of 160 cases. Hepatogastroenterology 55:2184–7.
- [13] Ali MA, Carroll KT, Rennert RC, et al. (2016). Stereotactic laser ablation as treatment for brain metastases that recur after

- stereotactic radiosurgery: a multiinstitutional experience. *Neurosurg Focus* 41:E11. PubMed PMID: 27690654.
- [14] Latorre M, Rinaldi C. (2009). Applications of magnetic nanoparticles in medicine: magnetic fluid hyperthermia. *P R Health Sci J* 28:227–38.
- [15] Tseng HY, Lee GB, Lee CY, *et al.* (2009). Localised heating of tumours utilising injectable magnetic nanoparticles for hyperthermia cancer therapy. *IET Nanobiotechnol* 3:46–54.
- [16] Hynynen K, Darkazanli A, Unger E, *et al.* (1993). MRI-guided non-invasive ultrasound surgery. *Med Phys* 20:107–15.
- [17] Ebbini ES, Ter Haar G. (2015). Ultrasound-guided therapeutic focused ultrasound: current status and future directions. *Int J Hyperthermia* 31:77–89.
- [18] Maloney E, Hwang JH. (2015). Emerging HIFU applications in cancer therapy. *Int J Hyperthermia* 31:302–9.
- [19] Leksell L. (1951). The stereotaxic method and radiosurgery of the brain. *Acta Chir Scand* 102:316–19.
- [20] Blomgren H, Lax I, Naslund I, *et al.* (1995). Stereotactic high dose fraction radiation therapy of extracranial tumors using an accelerator. Clinical experience of the first thirty-one patients. *Acta Oncol* 34:861–70.
- [21] Papiez L, Timmerman R, DesRosiers C, *et al.* (2003). Extracranial stereotactic radioablation: physical principles. *Acta Oncol* 42:882–94.
- [22] Timmerman R, Papiez L, McGarry R, *et al.* (2003). Extracranial stereotactic radioablation: results of a phase I study in medically inoperable stage I non-small cell lung cancer. *Chest* 124:1946–55.
- [23] Dieterich S, Ford E, Pavord D, *et al.* (2015). Practical radiation oncology physics: a companion to gunderson and tepper's clinical radiation oncology. Philadelphia(PA): Elsevier - Health Sciences Division.
- [24] Gunderson LL, Willett CG, Calvo FA, *et al.* (2011). Intraoperative irradiation: techniques and results: New York (NY): Humana Press.
- [25] Dewey WC, Holahan EV. (1984). Hyperthermia-basic biology. *Prog Exp Tumor Res* 28:198–219.
- [26] Overgaard J. (1982). Influence of sequence and interval on the biological response to combined hyperthermia and radiation. *Natl Cancer Inst Monogr* 61:325–32.
- [27] Kosterev VV, Kramer-Ageev EA, Mazokhin VN, *et al.* (2015). Development of a novel method to enhance the therapeutic effect on tumours by simultaneous action of radiation and heating. *Int J Hyperthermia* 31:443–52.
- [28] Gillette EL. (1984). Clinical use of thermal enhancement and therapeutic gain for hyperthermia combined with radiation or drugs. *Cancer Res* 44:4836s–41s.
- [29] Dewhirst MW, Sim DA. (1984). The utility of thermal dose as a predictor of tumor and normal tissue responses to combined radiation and hyperthermia. *Cancer Res* 44:4772s–80s.
- [30] Overgaard J. (1984). Formula to estimate the thermal enhancement ratio of a single simultaneous hyperthermia and radiation treatment. *Acta Radiol Oncol* 23:135–9.
- [31] Valdagni R, Amichetti M. (1994). Report of long-term follow-up in a randomized trial comparing radiation therapy and radiation therapy plus hyperthermia to metastatic lymph nodes in stage IV head and neck patients. *Int J Radiat Oncol Biol Phys* 28:163–9.
- [32] Huilgol NG, Gupta S, Sridhar CR. (2010). Hyperthermia with radiation in the treatment of locally advanced head and neck cancer: a report of randomized trial. *J Cancer Res Ther* 6:492–6.
- [33] Overgaard J, Gonzalez Gonzalez D, Hulshof MC, *et al.* (1996). Hyperthermia as an adjuvant to radiation therapy of recurrent or metastatic malignant melanoma. A multicentre randomized trial by the European Society for Hyperthermic Oncology. *Int J Hyperthermia* 12:3–20.
- [34] Vernon CC, Hand JW, Field SB, *et al.* (1996). Radiotherapy with or without hyperthermia in the treatment of superficial localized breast cancer: results from five randomized controlled trials. *Int J Radiat Oncol Biol Phys* 35:731–44.
- [35] Sneed PK, Stauffer PR, McDermott MW, *et al.* (1998). Survival benefit of hyperthermia in a prospective randomized trial of brachytherapy boost +/- hyperthermia for glioblastoma multiforme. *Int J Radiat Oncol Biol Phys* 40:287–95.
- [36] van der Zee J, González D, van Rhoon GC, *et al.* (2000). Comparison of radiotherapy alone with radiotherapy plus hyperthermia in locally advanced pelvic tumours: a prospective, randomised, multicentre trial. *Lancet* 355:1119–25.
- [37] Harima Y, Nagata K, Harima K, *et al.* (2001). A randomized clinical trial of radiation therapy versus thermoradiotherapy in stage IIIB cervical carcinoma. *Int J Hyperthermia* 17:97–105.
- [38] Jones EL, Oleson JR, Prosnitz LR, *et al.* (2005). Randomized trial of hyperthermia and radiation for superficial tumors. *J Clin Oncol* 23:3079–85.
- [39] Vasanthan A, Mitsumori M, Park JH, *et al.* (2005). Regional hyperthermia combined with radiotherapy for uterine cervical cancers: a multi-institutional prospective randomized trial of the international atomic energy agency. *Int J Radiat Oncol Biol Phys* 61:145–53.
- [40] Mitsumori M, Zeng ZF, Oliynychenko P, *et al.* (2007). Regional hyperthermia combined with radiotherapy for locally advanced non-small cell lung cancers: a multi-institutional prospective randomized trial of the International Atomic Energy Agency. *Int J Clin Oncol* 12:192–8.
- [41] Schroeder C, Gani C, Lamprecht U, *et al.* (2012). Pathological complete response and sphincter-sparing surgery after neoadjuvant radiochemotherapy with regional hyperthermia for locally advanced rectal cancer compared with radiochemotherapy alone. *Int J Hyperthermia* 28:707–14.
- [42] Mallory M, Gogineni E, Jones GC, *et al.* (2016). Therapeutic hyperthermia: the old, the new, and the upcoming. *Crit Rev Oncol Hematol* 97:56–64.
- [43] Khan FM. (2014). The physics of radiation therapy. 5th ed. Philadelphia (PA): Wolters Kluwer Health.
- [44] Kirkpatrick JP, Meyer JJ, Marks LB. (2008). The linear-quadratic model is inappropriate to model high dose per fraction effects in radiosurgery. *Semin Radiat Oncol* 18:240–3.
- [45] Lepock JR. (2005). How do cells respond to their thermal environment? *Int J Hyperthermia* 21:681–7.
- [46] Mouratidis PX, Rivens I, ter Haar G. (2015). A study of thermal dose-induced autophagy, apoptosis and necroptosis in colon cancer cells. *Int J Hyperthermia* 31:476–88.
- [47] Sapareto SA, Dewey WC. (1984). Thermal dose determination in cancer therapy. *Int J Radiat Oncol Biol Phys* 10:787–800.
- [48] Park C, Papiez L, Zhang S, *et al.* (2008). Universal survival curve and single fraction equivalent dose: useful tools in understanding potency of ablative radiotherapy. *Int J Radiat Oncol Biol Phys* 70:847–52.
- [49] Kavanagh BD, Newman F. (2008). Toward a unified survival curve: in regard to Park *et al.* (*Int J Radiat Oncol Biol Phys* 2008;70:847–852) and Krueger *et al.* (*Int J Radiat Oncol Biol Phys* 2007;69:1262–1271). *Int J Radiat Oncol Biol Phys* 71:958–9.
- [50] Wang JZ, Huang Z, Lo SS, *et al.* (2010). A generalized linear-quadratic model for radiosurgery, stereotactic body radiation therapy, and high-dose rate brachytherapy. *Sci Transl Med* 2:39ra48.
- [51] Hanin LG, Zaider M. (2010). Cell-survival probability at large doses: an alternative to the linear-quadratic model. *Phys Med Biol* 55:4687–702.
- [52] Astrahan M. (2008). Some implications of linear-quadratic-linear radiation dose-response with regard to hypofractionation. *Med Phys* 35:4161.
- [53] Guerrero M, Li XA. (2004). Extending the linear-quadratic model for large fraction doses pertinent to stereotactic radiotherapy. *Phys Med Biol* 49:4825–35.
- [54] Garcia LM, Wilkins DE, Raaphorst GP. (2007). Alpha/beta ratio: a dose range dependence study. *Int. J. Radiat. Oncol. Biol. Phys* 67:587.
- [55] McDannold N, Zhang Y-Z, Power C, *et al.* (2013). Nonthermal ablation with microbubble-enhanced focused ultrasound close to the optic tract without affecting nerve function: laboratory investigation. *J Neurosurg* 119:1208–20.

- [56] Carlson DJ, Stewart RD, Semenenko VA, *et al.* (2009). Combined use of Monte Carlo DNA damage simulations and deterministic repair models to examine putative mechanisms of cell killing. *Radiat Res* 169:447–59.
- [57] Viglianti BL, Dewhirst MW, Abraham JP, *et al.* (2014). Rationalization of thermal injury quantification methods: application to skin burns. *Burns* 40:896–902.
- [58] Elias WJ, Huss D, Voss T, *et al.* (2013). A pilot study of focused ultrasound thalamotomy for essential tremor. *N Engl J Med* 369:640–8.
- [59] Rieke V, Butts Pauly K. (2008). MR thermometry. *J Magn Reson Imag* 27:376–90.
- [60] Kondziolka D, Ong JG, Lee JY, *et al.* (2008). Gamma Knife thalamotomy for essential tremor. *J Neurosurg* 108:111–17.
- [61] Dewey W, Hopwood L, Sapareto S, *et al.* (1977). Cellular responses to combinations of hyperthermia and radiation. *Radiology* 123:463–74.
- [62] Raaphorst GP, Szekely J, Lobreau A, *et al.* (1983). A comparison of cell killing by heat and/or X rays in Chinese hamster V79 cells, Friend erythroleukemia mouse cells, and human thymocyte MOLT-4 cells. *Radiat Res* 94:340–9.
- [63] Flentje M, Flentje D, Sapareto SA. (1984). Differential effect of hyperthermia on murine bone marrow normal colony-forming units and AKR and L1210 leukemia stem cells. *Cancer Res* 44:1761–6.
- [64] Armour EP, McEachern D, Wang Z, *et al.* (1993). Sensitivity of human cells to mild hyperthermia. *Cancer Res* 53:2740–4.
- [65] Raaphorst GP, Feeley MM. (1994). Hyperthermia radiosensitization in human glioma cells comparison of recovery of polymerase activity, survival, and potentially lethal damage repair. *Int J Radiat Oncol Biol Phys* 29:133–9.
- [66] Lepock JR. (2003). Cellular effects of hyperthermia: relevance to the minimum dose for thermal damage. *Int J Hyperthermia* 19:252.
- [67] Scheenstra AEH, Rossi MMG, Belderbos JSA, *et al.* (2014). Alpha/beta ratio for normal lung tissue as estimated from lung cancer patients treated with stereotactic body and conventionally fractionated radiation therapy. *Int J Radiat Oncol Biol Phys* 88:224.
- [68] Williams MV, Denekamp J, Fowler JF. (1985). A review of alpha/beta ratios for experimental tumors: implications for clinical studies of altered fractionation. *Int J Radiat Oncol Biol Phys* 11:87.
- [69] Hynynen K, Colucci V, Chung A, *et al.* (1996). Noninvasive arterial occlusion using MRI-guided focused ultrasound. *Ultrasound Med Biol* 22:1071–7.
- [70] Abbas G, Schuchert MJ, Pennathur A, *et al.* (2007). Ablative treatments for lung tumors: radiofrequency ablation, stereotactic radiosurgery, and microwave ablation. *Thorac Surg Clin* 17:261–71.
- [71] Dewhirst MW, Lora-Michiels M, Viglianti BL, *et al.* (2003). Carcinogenic effects of hyperthermia. *Int J Hyperthermia* 19:236–51.
- [72] Fry W, Mosberg W, Barnard J, Fry F. (1954). Production of focal destructive lesions in the central nervous system with ultrasound. *J Neurosurg* 11:471–8.
- [73] Yarmolenko PS, Moon EJ, Landon C, *et al.* (2011). Thresholds for thermal damage to normal tissues: an update. *Int J Hyperthermia* 27:320–43.
- [74] Dewey W. (1994). Arrhenius relationships from the molecule and cell to the clinic. *Int J Hyperthermia* 10:457–83.
- [75] Foley JL, Eames M, Snell J, *et al.* (2013). Image-guided focused ultrasound: state of the technology and the challenges that lie ahead. *Imaging Med* 5:357–70.
- [76] Solazzo S, Mertyna P, Peddi H, *et al.* (2008). RF ablation with adjuvant therapy: comparison of external beam radiation and liposomal doxorubicin on ablation efficacy in an animal tumor model. *Int J Hyperthermia* 24:560–7.
- [77] Horkan C, Dalal K, Coderre JA, *et al.* (2005). Reduced tumor growth with combined radiofrequency ablation and radiation therapy in a rat breast tumor model 1. *Radiology* 235:81–8.
- [78] Grieco CA, Simon CJ, Mayo-Smith WW, *et al.* (2006). Percutaneous image-guided thermal ablation and radiation therapy: outcomes of combined treatment for 41 patients with inoperable stage I/II non-small-cell lung cancer. *J Vasc Interv Radiol* 17:1117–24.
- [79] Chan MD, Dupuy DE, Mayo-Smith WW, *et al.* (2011). Combined radiofrequency ablation and high-dose rate brachytherapy for early-stage non-small-cell lung cancer. *Brachytherapy* 10:253–9.
- [80] Imada H, Nomoto S, Tomimatsu A, *et al.* (1999). Local control of non-small cell lung cancer by radiotherapy combined with high power hyperthermia using an 8 MHz RF capacitive heating device. *Jpn J Hyperthermic Oncol* 15:19–24.
- [81] Anscher MS, Samulski TV, Dodge R, *et al.* (1997). Combined external beam irradiation and external regional hyperthermia for locally advanced adenocarcinoma of the prostate. *Int J Radiat Oncol Biol Phys* 37:1059–65.
- [82] Lindquist C, Paddick I. (2007). The Leksell Gamma Knife Perfexion and comparisons with its predecessors. *Neurosurgery* 61:130–40.
- [83] Livraghi T, Mueller PR, Silverman SG. (2008). Tumor ablation: principles and practice. In: van Sonnenberg E, McMullen W, Solbiati L, eds. New York (NY): Springer Science and Business Media.
- [84] Lagendijk J, Schellekens M, Schipper J, *et al.* (1984). A three-dimensional description of heating patterns in vascularised tissues during hyperthermic treatment. *Phys Med Biol* 29:495.
- [85] Barranco SC, Romsdahl MM, Humphrey RM. (1971). The radiation response of human malignant melanoma cells grown in vitro. *Cancer Res* 31:830–3.
- [86] Aubry JF, Tanter M, Pernot M, *et al.* (2003). Experimental demonstration of noninvasive transskull adaptive focusing based on prior computed tomography scans. *J Acoust Soc Am* 113:84–93.
- [87] Clement G, Hynynen K. (2002). A non-invasive method for focusing ultrasound through the human skull. *Phys Med Biol* 47:1219–36.
- [88] Moskvin V, Timmerman R, Fau - DesRosiers C, *et al.* (2004). Monte carlo simulation of the Leksell Gamma Knife: II. Effects of heterogeneous versus homogeneous media for stereotactic radiosurgery. *Phys Med Biol* 49:4879–95.
- [89] Rosner GL, Clegg ST, Prescott DM, *et al.* (1996). Estimation of cell survival in tumours heated to nonuniform temperature distributions. *Int J Hyperthermia* 12:223–39.
- [90] Hong ZY, Song KH, Yoon JH, *et al.* (2015). An experimental model-based exploration of cytokines in ablative radiation-induced lung injury in vivo and in vitro. *Lung* 193:409–19.
- [91] Kahn J, Tofilon PJ, Camphausen K. (2012). Preclinical models in radiation oncology. *Radiat Oncol* 7:223.
- [92] Pearce JA. (2013). Comparative analysis of mathematical models of cell death and thermal damage processes. *Int J Hyperthermia* 29:262–80.
- [93] Griffin RJ, Dings RP, Jamshidi-Parsian A, *et al.* (2010). Mild temperature hyperthermia and radiation therapy: role of tumour vascular thermotolerance and relevant physiological factors. *Int J Hyperthermia* 26:256–63.
- [94] Song CW, Shakil A, Griffin RJ, *et al.* (1997). Improvement of tumor oxygenation status by mild temperature hyperthermia alone or in combination with carbogen. *Semin Oncol* 24:626–32.
- [95] Liang P, MacRae TH. (1997). Molecular chaperones and the cytoskeleton. *J Cell Sci* 110:1431–40.
- [96] Pratt WB, Silverstein AM, Galigniana MD. (1999). A model for the cytoplasmic trafficking of signalling proteins involving the hsp90-binding immunophilins and p50cdc37. *Cellular Signal* 11:839–51.
- [97] Ling CC, Robinson E. (1988). Moderate hyperthermia and low dose rate irradiation. *Radiat Res* 114:379–84.
- [98] Sapareto SA, Hopwood LE, Dewey WC, Raju MR, Gray JW. (1978). Effects of hyperthermia on survival and progression of Chinese hamster ovary cells. *Cancer Res* 38:393.